Molecular Machines

Deutsche Ausgabe: DOI: 10.1002/ange.201607886
Internationale Ausgabe: DOI: 10.1002/anie.201607886

Thermally Induced Intra-Carboxyl Proton Shuttle in a Molecular Rack-and-Pinion Cascade Achieving Macroscopic Crystal Deformation

*You-Gui Huang, Yoshihito Shiota, Sheng-Qun Su, Shu-Qi Wu, Zi-Shuo Yao, Guo-Ling Li, Shinji Kanegawa, Soonchul Kang, Takashi Kamachi, Kazunari Yoshizawa, Katsuhiko Ariga, and Osamu Sato**

Abstract: *Proton transport via dynamic molecules is ubiquitous in chemistry and biology. However, its use as a switching mechanism for properties in functional molecular assemblies is far less common. In this study, we demonstrate how an intra-carboxyl proton shuttle can be generated in a molecular assembly akin to a rack-and-pinion cascade via a thermally induced single-crystal-to-single-crystal phase transition. In a triply interpenetrated supramolecular organic framework (SOF), a 4,4′-azopyridine (azpy) molecule connects to two biphenyl-3,3′,5,5′-tetracarboxylic acid (H_4BPTC) molecules to form a functional molecular system with switchable mechanical properties. A temperature change reversibly triggers a molecular movement akin to a rack-and-pinion cascade, which mainly involves 1) an intra-carboxyl proton shuttle coupled with tilting of the azo molecules and azo pedal motion and 2) H_4BPTC translation. Moreover, both the molecular motions are collective, and being propagated across the entire framework, leading to a macroscopic crystal expansion and contraction.*

Long-distance proton transport is ubiquitous in chemistry and biology[1–4] and plays a crucial role in a variety of chemical and biological activities including viral replication,[5] proton pumping through membrane protein channels,[6] and the removal of acetyl moieties from histone tails.[7] For example, proton conduction in influenza M2 proton channels is regulated by a proton-shuttling process that is dynamically assisted by an imidazolium ring flip; this process represents a key step in virus replication.[8] Proton transport in these systems is facilitated by hydrogen-bonded networks that serve as proton conduits through which the proton relay via the Grotthuss and/or vehicle mechanisms.[9–12] Although replicating the functions of these biological systems in synthetic materials is extremely challenging, great achievements have been accomplished by building prototypes that can mimic the complicated ion-transport pathways of biological systems.[13–17] For example, the coordination-coupled proton relay process that is important in histidine residues[18,19] has been replicated in some types of hydrazine-based rotary switches.[14,15] Moreover, carboxyl groups can ionize under the right conditions, releasing the proton from the hydroxy group with the negative charge "flip-flopping" back and forth between the two oxygen atoms. Reversely, the ionized carboxyl groups can be protonated with the assistance of a stronger acid.[20] This characteristic makes it possible to initiate an intra-carboxyl proton shuttle using a dynamic molecule.

Therefore, we synthesized a supramolecular organic framework (SOF) comprising of 4,4′-azopyridine (azpy) and biphenyl-3,3′,5,5′-tetracarboxylic acid (H_4BPTC) to generate a molecular assembly akin to a rack-and-pinion cascade. H_4BPTC can form hydrogen bonds with azpy molecules. Moreover, ethylene and azo groups are both well-known to undergo pedal motion,[21–24] which may result in fine modulation of the electronic structures of ethylene or azo-based molecules.[25] The ethylene group has been used to build a molecular machine akin to rack-and-pinion gears.[21] Therefore, we envisaged that the pyridine moiety in azpy may serve as a proton acceptor and facilitate proton transfer in the carboxyl group.

Herein, we show that an SOF comprising azpy and H_4BPTC molecules undergoes a thermally induced intra-carboxyl proton shuttle in a single-crystal to single-crystal manner. All molecular motions in the phase transition are collective and are propagated throughout the single crystal, leading to macroscopic crystal expansion and contraction. To the best of our knowledge, this is the first example of breathing motion in a wine-rack-type framework resulting from a single-crystal to single-crystal phase transition, wherein proton shuttling via a dynamic molecule plays a key role.

The supramolecular framework $[(H_4BPTC)(azpy)_2]_n$ (**1**) was obtained via cocrystallization of H_4BPTC and azpy in methanol. Single-crystal X-ray crystallography at 333 K revealed that compound **1** crystallizes in the centrosymmetric space group *C*2/*c* (Tables S1 and S2 in the Supporting Information) with a triply-interpenetrated supramolecular framework structure (Figure S1b). The asymmetric unit contains an azpy molecule and half a H_4BPTC molecule (Figure 1 b). The azo group of the azpy molecule is disordered over two sites with occupancies of 0.80 and 0.20, and the populations of the two conformers change with temperature, implying dynamic disorder (site occupancies found at 363 K: 0.75 and 0.25)[26] (Table S3). Therefore, the azpy molecules

[*] Dr. Y.-G. Huang, Y. Shiota, S.-Q. Su, S.-Q. Wu, Z.-S. Yao, G.-L. Li, S. Kanegawa, S. Kang, T. Kamachi, K. Yoshizawa, Prof. O. Sato
Institute for Materials Chemistry and Engineering, Kyushu University
744 Motooka Nishi-ku, Fukuoka, 819-0395 (Japan)
E-mail: sato@cm.kyushu-u.ac.jp
Dr. Y.-G. Huang, Prof. K. Ariga
World Premier International (WPI) Center for Materials Nanoarchitectonics (MANA), Institute for Materials Science (NIMS)
1-1 Namiki, Tsukuba, Ibaraki, 305-0044 (Japan)

Supporting information for this article can be found under: http://dx.doi.org/10.1002/anie.201607886.

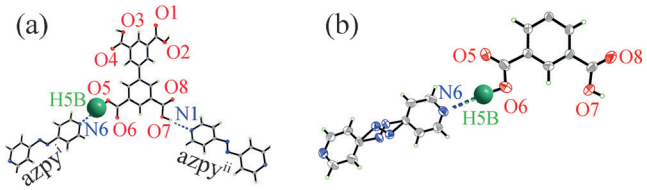

Figure 1. The asymmetric unit of a) the LT phase and b) the HT phase of compound **1**. ORTEP drawing at 30% probability. The green sphere represents the transported proton in the phase transition.

undergo a conformation interconversion via azo-pedal-motion in this phase of the crystal. The dihedral angles between the two phenyl rings in the H_4BPTC molecule (φ) and the two pyridyl rings in the azpy molecule (α) are 32.2° and 13.2° (Table S4), respectively. Each H_4BPTC connects to its four neighbors by azpy by two kinds of hydrogen bonds (O-H···N: 2.713–2.792 Å) forming a (4,4) two-dimensional (2D) structure (Tables S5 and S6). A rhombic grid with a hinged angle θ of 79.7°, which is formed by four H_4BPTC and four azpy molecules, is the basic building unit in the 2D structure (Figures 2b and 3c). This grid is akin to a framework with

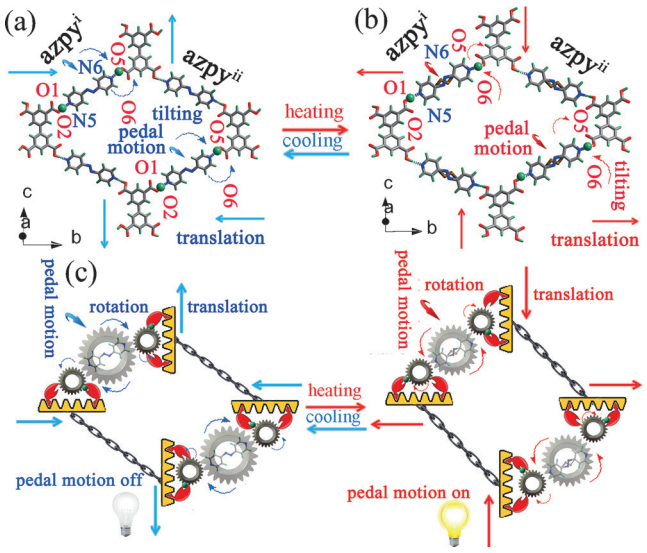

Figure 2. a, b) The structural reorganization of the rhombic grid in compound **1** during the phase transition. c) Schematic of the rack-and-pinion cascade movement achieving the intra-carboxyl proton shuttle in compound **1**. The green spheres represent the transported protons, and the minor conformers of azo groups in the HT phase are highlighted in yellow.

a "wine-rack" topology.[27] In the rhombic grid, the azpy molecules act as the sides and bridge the H_4BPTC molecules as vertices with an angle of 109.8° to the shorter diagonal of the rhombic grid (δ) (Table S4 and Figures 3c, S2d). Because of the large cavities present in each single framework, three identical frameworks triply interpenetrate parallely to form a dense framework, in which each rhombic grid crosses its eight neighbors from the other two single frameworks twice (Figure S1b).

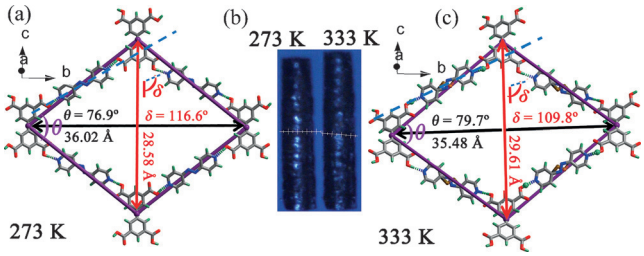

Figure 3. a, c) Structural presentation of the deformation of the rhombic grid in compound **1** in the phase transition. b) Crystal photographs showing significant crystal expansion or contraction in the phase transition.

Thermogravimetric analysis (TGA) showed that compound **1** decomposes at ca. 440 K (Figure S3). Differential scanning calorimetry (DSC) curves showed a multistep reversible phase transition at a temperature far lower than the decomposition point (Figure 4b). The reversible phase

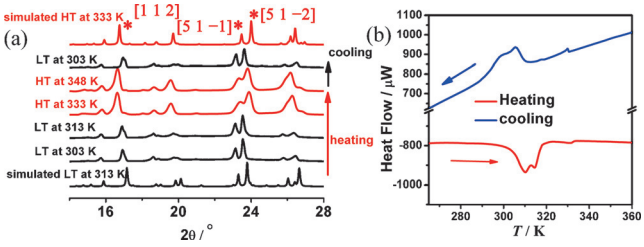

Figure 4. a) PXRD pattern evolution of compound **1** showing the reversible phase transition, b) DSC curves of compound **1** showing the reversible multistep phase transition.

transition is supported by variable-temperature powder X-ray diffraction (PXRD) and IR spectra (Figures 4a and S4). In the PXRD patterns, the peaks indexed to [1 1 2], [5 1 −1], and [5 1 −2] exhibited significant and reversible shifts near the phase transition temperature (Figure 4a). To further elucidate the structural dynamics of compound **1** during the reversible phase transition, variable-temperature crystal structure determinations were performed in the range 123–363 K. The unit cell parameters undergo an abrupt change at the phase transition temperature (Figures S2a, S2b). During the phase transition, thermal expansion along the *a* and *b* axes was negative, an exceptionally large positive thermal expansion occurred along the *c* axis. This exceptionally large anisotropic thermal expansion can be rationalized by systematically comparing the crystal structures at 333 K and 273 K.

The structure of compound **1** was found to transition to a low-temperature (LT) phase below 273 K; this phase belongs to the noncentrosymmetric space group *Cc* (Tables S1 and S2), implying that a symmetry breaking process had occurred (Figure S5). In comparison with the high-temperature (HT) phase, the asymmetric unit of the LT phase is doubled, containing one H_4BPTC and two azpy molecules denoted as azpy^{i} and azpy^{ii}, respectively (Figure 1a). The structure of the LT phase is also a triply interpenetrated supramolecular framework based on rhombic

grids (Figures 2a, S1a, S6), but the geometries of the rhombic grids in the two phases are quite different. In response to the temperature change, the structural reorganizations of the rhombic grid primarily proceeded through two motions: 1) intra-carboxyl proton shuttle coupled with tilting of azo molecules and azo-pedal-motion, and 2) H_4BPTC translation (Figure 2). Accompanying these motions, the configurations of both H_4BPTC and azpy changed slightly (Figures S2c and S7). These molecular motions lead to a symmetry breaking (i.e., the total symmetry decreases from four symmetry operations (E, i, C_2, σ_h) to two (E, σ_h)). The 2_1-fold axis and the inversion center i disappear in the LT phase (Figure S5). The phase transition occurs in a manner of reversible single-crystal to single-crystal with an Aizu notation of 2/*mFm*.[28] Structural determinations were performed on a single crystal of compound **1** heated from 123 K to 363 K and then cooled back to 123 K. The crystallographic data quality of the LT phase was not affected by the thermal cycle (Tables S1 and S2).

As shown in Figures 2 and 3, in the rhombic grid of the HT phase, all four of the azpy molecules are symmetry related and their azo groups are undergoing pedal motion. After the phase transition, the disorder disappeared, implying that the azo pedal motion was switched off in the LT phase. The N=N bonds of the major conformers of azpy^{i} and azpy^{ii} are approximately parallel with center-to-center distances of 18.19 Å in the HT phase, while in the LT phase, the N=N bonds are in a criss-crossed arrangement with a twist angle of 59.6° and a center-to-center distance of 14.83 Å. Because of the phase transition, the C_2 symmetry related azpy^{i} and azpy^{ii} molecules present in the HT phase became crystallographically independent in the LT phase. To accommodate this movement, the configurations of both azpy^{i} and azpy^{ii} slightly changed with the dihedral angles (α and γ) between the pyridyl rings changing from a common value of 13.2° to 16.8° and 7.5°, respectively (Figure S2c and Table S4).

In addition to the on-off switching of azo-pedal-motion, the azpy^{i} molecules were also significantly reoriented in the plane of the rhombic grid, with the angle (δ) changing from 109.8° at 333 K to 116.6° at 273 K (Figures 3, S2d, and Table S4). The H_4BPTC molecules underwent a translation along the diagonals of the rhombic grid (Figures 2 and 3). As a result, the rhombic grid "breathed" like a wine-rack in response to the temperature change. From 333 K to 273 K, the longer diagonal expanded by 1.52% resulting in the ca. 1.53% expansion of the b axis and the shorter diagonal contracted by 3.48% resulting in the ca. 3.21% contraction of the c axis (Figures 3 and S2a). The large anisotropic thermal expansion is comparable to those of some other molecular crystals that show significant crystal deformation in their phase transitions.[29,30] Accompanying the translation, the phenyl rings in the H_4BPTC molecules rotated slightly, with the angle φ increasing from 32.2° at 333 K to 35.0° at 273 K (Figure S2c and Table S4). The dihedral angles between the carboxylic acid groups of H_4BPTC and their parent phenyl rings also changed from 9.7°, 9.7°, 14.7°, and 14.7° at 333 K to 3.1°, 13.7°, 15.3°, and 17.6° at 273 K, respectively. The LT phase shows a large anisotropic thermal expansion in the range 123–313 K (Table S7).

Furthermore, it is interesting that intra-carboxyl proton shuttle is achieved by the phase transition. As shown in Figure 2, azpy^{i} is hydrogen bonded to O1 and O6 in the HT phase, while it is hydrogen bonded to O2 and O5 in the LT phase. This implies that intra-carboxyl electron-coupled proton transfer occurred during the phase transition, provided that the carboxylic groups are protonated in both phases. Although a difference Fourier analysis yielded nominal H-atom positions, both near O atoms (Figures S8–S13), the electron density of H atoms is usually too small to allow an accurate determination of their positions. Nevertheless, an alternative means of determining whether a carboxylic group is protonated or not is to scrutinize its local π molecular geometry.[31] It is well known that deprotonation of a carboxylic group leads to delocalization in the π-electron system such that the C=O (≈1.21 Å) and C–O (≈1.31 Å) bonds change to two identical C=O bonds (≈1.25 Å).[32,33] The C–O bond lengths can be obtained with sufficient accuracy to discriminate between the protonated and deprotonated carboxylic groups in case that no structural disorder exists in the carboxylic groups. As shown in Table 1, both carboxylic groups (C7-O1-O2 and C16-O5-O6) that hydrogen bond to azpy^{i} show characteristics of protonation in both phases, and each single and double bond "pair" interchanged before and after the phase transition. These characterizations indicate that the hydrogen bonds between azpy^{i} and H_4BPTC are neutral O-H···N hydrogen bonds in both phases. Protons reside on the O1 and O6 atoms in the HT phase and on the O2 and O5 atoms in the LT phase.

Table 1: Bond lengths [Å] of carboxyl groups in H_4BPTC for compound **1** LT phase at 273 K and compound **1** HT phase at 333 K.

Bond (LT phase)			
C7–O1	1.199(6)	C15–O7	1.303(6)
C7–O2	1.327(6)	C15–O8	1.214(6)
C8–O3	1.306(6)	C16–O5	1.301(6)
C8–O4	1.214(6)	C16–O6	1.216(6)
Bond (HT phase)[a]			
C7–O1	1.301(5)	C15–O7	1.301(5)
C7–O2	1.201(5)	C15–O8	1.201(5)
C8–O3	1.295(5)	C16–O5	1.221(5)
C8–O4	1.221(5)	C16–O6	1.295(5)

[a] The atoms are labeled in accordance with those in the LT phase. Intra-carboxyl proton shuttles occurred in the C7-O1-O2 and C16-O5-O6 two carboxylic acid groups during the phase transition.

In order to get insights into the phase transition, density functional theory (DFT) calculations were performed at the B3LYP/6-31G** level of theory. The energy barriers for the molecular motions which may occur in the phase transition were calculated. Two possible pathways for intra-carboxyl proton transfer, i.e., 1) direct proton hopping between two carboxyl O atoms and 2) proton relay via the pyridyl N atom of azpy, were compared (Figure S14). The direct proton-hopping pathway has a very high activation barrier (33 kcal mol^{-1}) (Tables S14 and S15). In contrast, the activation barrier for the proton relay pathway is much smaller at

18 kcal mol^{-1} (Tables S16 and S17). Therefore, for the phase transition in compound **1**, the proton relay pathway is energetically preferred. The presence of the azpy with pyridyl N atom facilitates the intra-carboxyl proton transfer. Based on the results of the DFT calculations, we may propose a reasonable pathway as shown in Figure S15 (Tables S18–S22). Proton migration coupled with tilting of azo molecules and azo-pedal-motion occurred in the phase transition with transition states of 18 kcal mol^{-1}, and on–off switching of azo-pedal motion was achieved. Notably, the pedal motion of neutral azpy involves an energy barrier of 9.9 kcal mol^{-1}, while that of diprotonated azpy (H_2azpy^{2+}) is only 6.7 kcal mol^{-1} (Figure S16 and Tables S10–S13). This result suggests that ionization of the carboxyl groups can kinetically assist the azo pedal motion.

We successfully synthesized compound **1**-d_4 $[(D_4BPTC)(azpy)_2]_n$ which is isostructural to the HT phase of compound **1** (Table S9 and Figures S16, S17). For compound **1**-d_4, single-crystal X-ray crystallography and DSC showed no phase transition in the range 123–393 K (Table S8 and Figures S19, S20). This substantial isotope effect implies that the protons of the carboxyl groups do play an important role in the phase transition of compound **1**, hence supporting the proposed proton relay mechanism,[34–36] The populations of the two azpy conformers in compound **1**-d_4 also vary with temperature (Table S3), which further indicates the dynamic disorder of azpy observed in the HT phase of compound **1**. The pedal motion of neutral azpy molecules in compound **1**-d_4 was switched off at 123 K much lower than that in compound **1** (Figure S21). Therefore, the phase transition in compound **1** enormously raised the azo-pedal-motion off temperature from 123 K to 313 K. Unlike the LT phase of compound **1**, all of the three crystallographic axes of compound **1**-d_4 show positive thermal expansion in the range 123–373 K (Table S9 and Figure S19).

Although azo-pedal-motion, molecular tilting, and the breathing of the wine-rack-type grids are not rare in the crystal structure transformations,[27,29,37–39] in this case, all of the three movements have been observed in the same crystal. In addition, intra-carboxyl proton shuttle was realized by the molecular movements. Moreover, the molecular aggregate of azpy^i with its two adjacent H_4BPTC molecules can be considered as an analog to a rack-and-pinion cascade at the molecular level. In this molecular assembly, an azpy^i molecule with two transported protons acts as the pinion cascade that experiences rotation movement. Because of the hydrogen bonds between azpy^i and H_4BPTC, the rotation of the cascade pinion gear supports a correlated translation of two H_4BPTC rack gears, resulting in the conversion of rotary motion to linear motion (Figure 2c).

Harnessing molecular motion to yield reversible macroscopic crystal shape change is a fascinating and challenging subject in crystal engineering.[29,30,40–42] All the molecular motions observed in the rhombic grid of compound **1** are collective, being propagated throughout the whole 2D supramolecular framework leading to the breathing observed in the framework. Remarkably, this breathing can be converted into a macroscopic change in the crystal shape (Figure 3b). The deformation process of a single crystal was monitored by a microscope equipped with a heating-and-cooling stage. A single crystal ($\approx 0.05\,mm \times 0.30\,mm \times 1.65\,mm$) contracted or expanded about 4% along its long axis (Figure 3b) during cooling or heating in the range 273–333 K. The magnitude of the expansion is consistent with the change observed crystallographically in the *c* axis. Furthermore, the crystal exhibited no evidence of appreciable fatigue after five cycles (Figure S22). The reversible expansion and contraction processes of a single crystal up to 1.82 mm in length in the range 123–333 K were recorded on two videos (Supporting Information).

In conclusion, an intra-carboxyl proton shuttle, which is facilitated by the presence of azo molecules with pyridine ring, has been observed for the first time in the thermally induced, multistep single-crystal-to-single-crystal phase transition of a supramolecular framework. The phase transition involves proton migration, which is coupled with azo-pedal motion, a change in orientation of azo molecules, and displacement of H_4BPTC molecules. All the motions are collective and are propagated throughout the framework, leading to the macroscopic expansion and contraction of the crystal. These observations may provide some valuable insights into the design of materials that can replicate the functions of biological systems. The macroscopic change in the crystal shape harnessed by molecular movements promises a wide range of potential applications in the production of thermal actuators and artificial muscle.

Acknowledgements

Y.-G.H. thanks the Japan Society for the Promotion of Science for a postdoctoral fellowship (No. P13033). This work was supported by a JSPS KAKENHI Grant, number 16H00843.

Keywords: crystal deformation · molecular machine · phase transitions · proton shuttle

How to cite: *Angew. Chem. Int. Ed.* **2016**, *55*, 14628–14632
Angew. Chem. **2016**, *128*, 14848–14852

[1] a) R. J. P. Williams, *Annu. Rev. Biophys. Biophys. Chem.* **1988**, *17*, 71–97; b) O. Sato, *Nat. Chem.* **2016**, *8*, 644–656.
[2] J. F. Haw, T. Xu, J. B. Nicholas, P. W. Goguen, *Nature* **1997**, *389*, 832–835.
[3] C. Tanner, C. Manca, S. Leutwyler, *Science* **2003**, *302*, 1736–1739.
[4] D. F. Brougham, R. Caciuffo, A. J. Horsewill, *Nature* **1999**, *397*, 241–243.
[5] I. Belevich, M. I. Verkhovsky, M. Wikström, *Nature* **2006**, *440*, 829–832.
[6] S. D. Cady, W. B. Luo, F. Hu, M. Hong, *Biochemistry* **2009**, *48*, 7356–7364.
[7] H. Terao, T. Sugawara, Y. Kita, N. Sato, E. Kaho, S. Takeda, *J. Am. Chem. Soc.* **2001**, *123*, 10468–10474.
[8] F. Hu, W. B. Luo, M. Hong, *Science* **2010**, *330*, 505–508.
[9] A. K. Ghosh, G. B. Schuster, *J. Am. Chem. Soc.* **2006**, *128*, 4172–4173.
[10] C. J. T. de Grotthuss, *Ann. Chim.* **1806**, *58*, 54–73.

[11] K. D. Kreuer, A. Rabenau, W. Weppner, *Angew. Chem. Int. Ed. Engl.* **1982**, *21*, 208 – 209; *Angew. Chem.* **1982**, *94*, 212 – 212.
[12] S. Bureekaew, S. Horike, M. Higuchi, M. Mizuno, T. Kawamura, D. Tanaka, N. Yanai, S. Kitagawa, *Nat. Mater.* **2009**, *8*, 831 – 836.
[13] C. Costentin, M. Robert, J. M. Savéant, C. Tard, *Angew. Chem. Int. Ed.* **2010**, *49*, 3803 – 3806; *Angew. Chem.* **2010**, *122*, 3891 – 3894.
[14] X. Su, T. F. Robbins, I. Aprahamian, *Angew. Chem. Int. Ed.* **2011**, *50*, 1841 – 1844; *Angew. Chem.* **2011**, *123*, 1881 – 1884.
[15] D. Ray, J. T. Foy, R. P. Hughes, I. Aprahamian, *Nat. Chem.* **2012**, *4*, 757 – 762.
[16] O. H. Kwon, Y. S. Lee, B. K. Yoo, D. J. Jang, *Angew. Chem. Int. Ed.* **2006**, *45*, 415 – 419; *Angew. Chem.* **2006**, *118*, 429 – 433.
[17] C. D. Assouma, A. Crochet, Y. Chérémond, B. Giese, K. M. Fromm, *Angew. Chem. Int. Ed.* **2013**, *52*, 4682 – 4685; *Angew. Chem.* **2013**, *125*, 4780 – 4783.
[18] G. Feher, J. P. Allen, M. Y. Okamura, D. C. Rees, *Nature* **1989**, *339*, 111 – 116.
[19] M. Paddock, M. Graige, G. Feher, M. Okamura, *Proc. Natl. Acad. Sci. USA* **1999**, *96*, 6183 – 6188.
[20] A. D. McNaught, A. Wilkinson, *IUPAC Compendium of Chemical Terminology – the Gold Book, 2nd ed.*, Blackwell Scientific Publications, Oxford, **1997**.
[21] A. N. Sokolov, D. C. Swenson, L. R. MacGillivary, *Proc. Natl. Acad. Sci. USA* **2008**, *105*, 1794 – 1797.
[22] S. Ohba, H. Hosomi, Y. Ito, *J. Am. Chem. Soc.* **2001**, *123*, 6349 – 6352.
[23] J. Harada, H. Uekusa, Y. Ohashi, *J. Am. Chem. Soc.* **1999**, *121*, 5809 – 5810.
[24] K. M. Hutchins, R. H. Groeneman, E. W. Reinheimer, D. C. Swenson, L. R. MacGillivray, *Chem. Sci.* **2015**, *6*, 4717 – 4722.
[25] M. Emond, T. L. Saux, S. Maurin, J. Baudin, R. Plasson, L. Jullien, *Chem. Eur. J.* **2010**, *16*, 8822 – 8831.
[26] J. Harada, K. Ogawa, *Cryst. Growth Des.* **2014**, *14*, 5182 – 5188.
[27] A. U. Ortiz, A. Boutin, A. H. Fuchs, F. X. Coudert, *Phys. Rev. Lett.* **2012**, *109*, 195502.
[28] K. Aizu, *J. Phys. Soc. Jpn.* **1969**, *27*, 387 – 396.
[29] Z. S. Yao, M. Mito, T. Kamachi, Y. Shiota, K. Yoshizawa, N. Azuma, Y. Miyazaki, K. Takahashi, K. R. Zhang, T. Nakanishi, S. Kang, S. Kanegawa, O. Sato, *Nat. Chem.* **2014**, *6*, 1079 – 1083.
[30] S. Q. Su, T. Kamachi, Z. S. Yao, Y. G. Huang, Y. Shiota, K. Yoshizawa, N. Azuma, Y. Miyazaki, M. Nakano, G. Maruta, S. Takeda, S. Kang, S. Kanegawa, O. Sato, *Nat. Commun.* **2015**, *6*, 8810.
[31] S. Horiuchi, R. Kumai, Y. Tokura, *Angew. Chem. Int. Ed.* **2007**, *46*, 3497; *Angew. Chem.* **2007**, *119*, 3567-3451.
[32] C. C. Trout, J. D. Kubicki, *Geochim. Cosmochim. Acta* **2006**, *70*, 44 – 55.
[33] R. Chang, *Chemistry*, New York, McGraw-Hill, **1994**.
[34] L. Masgrau, A. Roujeinikova, L. O. Johannissen, P. Hothi, J. Basran, K. E. Ranaghan, A. J. Mulholland, M. J. Sutcliffe, N. S. Scrutton, D. Leys, *Science* **2006**, *312*, 237 – 241.
[35] Y. L. Lin, J. L. Gao, *J. Am. Chem. Soc.* **2011**, *133*, 4398 – 4403.
[36] S. Takeda, A. Tsuzumitani, *Chem. Phys. Lett.* **1992**, *198*, 316 – 320.
[37] W. Li, M. R. Probert, M. Kosa, T. D. Bennett, A. Thirumurugan, R. P. Burwood, M. Parinello, J. A. K. Howard, A. K. Cheetham, *J. Am. Chem. Soc.* **2012**, *134*, 11940 – 11943.
[38] K. Lekin, H. Phan, S. M. Winter, J. W. L. Wong, A. A. Leitch, D. Laniel, W. J. Yong, R. A. Secco, J. S. Tse, S. Desgreniers, *J. Am. Chem. Soc.* **2014**, *136*, 8050 – 8062.
[39] A. U. Ortiz, A. Boutin, A. H. Fuchs, F. X. Coudert, *J. Chem. Phys.* **2013**, *138*, 174703.
[40] M. A. Garcia-Garibay, *Angew. Chem. Int. Ed.* **2007**, *46*, 8945 – 8947; *Angew. Chem.* **2007**, *119*, 9103 – 9105.
[41] S. Kobatake, S. Takami, H. Muto, T. Ishikawa, M. Irie, *Nature* **2007**, *446*, 778 – 781.
[42] J. K. Sun, W. Li, C. Chen, C. X. Ren, D. M. Pan, J. Zhang, *Angew. Chem. Int. Ed.* **2013**, *52*, 6653 – 6657; *Angew. Chem.* **2013**, *125*, 6785 – 6789.

Received: August 12, 2016
Revised: September 19, 2016
Published online: October 13, 2016

